

MAGNETIC MEASUREMENTS OF THE NSLS-II INSERTION DEVICES

M. Musardo[#], D. Harder, C. A. Kitegi and T. Tanabe
 National Synchrotron Light Source II, Brookhaven National Laboratory
 Upton, New York 11973-5000, USA

Abstract

This paper presents the results and the recent progress in the magnetic measurements of the insertion devices (IDs) for the National Synchrotron Light Source-II (NSLS-II) at Brookhaven National Laboratory (BNL). A detailed analysis of the magnetic measurements is carried out for various IDs with particular attention at the influence of the magnetic field errors on the devices spectral performance. Several specific details of the measurements and the recent results from IDs commissioning are presented.

INTRODUCTION

The NSLS-II is a state-of-the-art electron storage ring of 3 GeV third generation light source at Brookhaven National Laboratory. NSLS-II has been designed and constructed to deliver photons with high average spectral brightness in the 2 keV to 10 keV energy range exceeding 10^{21} ph/s/0.1%bw/mm²/mrad², and high spectral flux exceeding 10^{15} ph/s/0.1%bw. This performance requires the storage ring to support a very high-current electron beam ($I = 500$ mA) with a very small horizontal (down to 0.5 nm-rad) and vertical (8 pm-rad) emittance. [1].

NSLS-II will be able to accommodate more than 60 beam-lines in the final built-out for a wide-range of scientific programs, with future development of additional beam-lines through canted insertion devices and multiple hutches [2].

At the time of this report 13 insertion devices have been installed into the storage ring and are currently under commissioning and studies [3,4]. All these IDs were procured as a “turn-key” devices from main ID companies (Danfysik, HITACHI and Kyma).

They include 6 damping wigglers (DWs), utilized to achieve a low horizontal beam emittance and as broadband sources of very bright and high flux x-rays superior to conventional bend-magnet sources, 2 Apple-II type undulator with four movable arrays, for full polarization control and 5 In-Vacuum Undulator for hard X-Ray. The basic parameters characterizing the NSLS-II IDs installed so far are listed in Table 1.

MAGNETIC FIELD MEASUREMENTS

All insertion devices mentioned above underwent rigorous magnetic measurements before installation into the storage ring in order to validate the ID performance

Work performed under the auspices of U.S. Department of Energy, under contract DE-SC0012704.
 #musardo@bnl.gov

requirements and confirm the measurement data of vendors. Furthermore some IVUs went through magnetic retuning performed at BNL with vendor technicians in order to improve the magnetic field quality.

Table 1: NSLS-II Insertion Devices Installed

Cell ID	Beam line	Type	Length [mm]	Period [mm]	B _{PEAK} [Tesla]	Gap [mm]
23	CSX1 CSX2	Apple II	4.0 (2x2)	49.0	0.57 (C)	11.5
					0.94 (V)	
					0.72 (H)	
					0.4 (45°)	
10	IXS	IVU	3.0	22.0	0.78	7.4
3	HXN	IVU	3.0	20.0	1.03	5.2
11	CHX	IVU	3.0	20.0	1.03	5.2
5	SRX	IVU	1.5	21.0	0.9	6.2
19	FMX	IVU	1.5	21.0	0.9	6.2
28	XPD PDF	Hybrid PM	6.8 (2x3.4)	100	1.8	15
8	ISS	Hybrid PM	6.8 (2x3.4)	100	1.8	15
18	FXI	Hybrid PM	6.8 (2x3.4)	100	1.8	15

Magnetic Measurement Facility

The magnetic measurement system facility at BNL consists in a 3D Hall probe-mapping bench MMB-6500 for local magnetic field measurement and an Integrated Field Measurement System (IFMS) for first and second field integral measurement [5]. The IFMS is a versatile measurement system as it includes 3 different field integral measurement systems, a stretch wire system, a flipping coil system and a long board. The flipping coil has been used to measure IDs field integral.

A fully integrated SENIS 3-axis ultra-low noise probe, accurately recalibrated [6], is used as Hall sensor in order to measure three independent components of the magnetic field at single location. The Hall sensors arranged along longitudinal axis have a magnetic field sensitive volume of $150 \times 1 \times 150 \mu\text{m}$, which allows very high-resolution measurements with a linearity error up to 2 T less of 0.15% and a good angular accuracy with an orthogonality error $< 2^\circ$.

The full control of the measurement system is carried out using a LabView software. Recent developments have allowed the automation of ID gap/phase motions and

measurement, shortening significantly the measurement time of an insertion device [7].

Magnetic Field Errors

The field errors, such as those arising from the magnetic imperfections of the magnet blocks but also of their dimensional, shape and positioning errors, distorting the periodicity of the field can significantly reduce the performance of the devices. Angular errors and magnetic inhomogeneities inside the magnet blocks as well as variations in magnetization strength from block to block all contribute to deform the ideal beam trajectory and to produce an undesirable deterioration of the quality of the emitted radiation. Thus, the measurement, localization, and correction of the field errors can be a critical issue.

The RMS phase error was introduced as a figure of merit of the undulator spectral performance and magnetic field quality [8]. It can be defined as the cumulative path length difference between the electron's actual trajectory of real device and an ideal trajectory, expressed in degrees of phase at the fundamental optical wavelength. It is calculated using the optical phase function as defined by the following:

$$\phi(z) = \frac{2\pi}{\lambda} \left[\frac{z}{2\gamma^2} + \int_{\frac{L}{2}}^z \frac{\beta_x^2(z') + \beta_y^2(z')}{2} dz' \right] \quad (1)$$

which describes the phase lag between an electron and the front of the emitted wave train directed along the nominal axis z . Where L is the total length of the undulator, γ the Lorentz factor of an electron moving in the undulator magnetic field, λ is the radiation wavelength, $\beta_{x,y}$ the horizontal/vertical relative velocity of the electron. The fundamental wavelength of the undulator radiation is such that over one magnet period λ_u the phase lag is 2π , and hence the emission adds constructively. Eq. 1 is calculated from the magnetic field measurements and evaluated every $\lambda_u/4$, at the point of radiation emission at each pole, which corresponds to the extreme value of the magnetic field B . The phase error is thus defined as the deviation of the sampling at $\lambda_u/4$ and the liner fit of the phase function.

Magnetic errors are responsible for non-zero first and second field integral along the beam axis. The first and second integrals defined in the NSLS-II Technical Specification are the following:

$$I(x) = \int_{-\infty}^{+\infty} B(z', x, y) dz' \quad (2)$$

$$J(x) = \int_{-\infty}^{+\infty} \int_{-\infty}^z B(z', x, y) dz' dz \quad (3)$$

$I(x)$ and $J(x)$ have been accurately measured in order to ensure that the integral multi-pole components are maintained within the specification requirements.

Magnetic Field Results

In order to improve the magnetic field quality in term of phase error and to reduce the field integral errors as

well as the multi-pole components, different in-house corrections have been carried out for two 1.5 m IVUs provided by Neomax. Final magnetic tuning have been performed also for two 2,8 m (currently under installation) and 3 m IVUs with Neomax technicians. Although the vendor's data were found satisfactory, the discrepancy between their magnetic field measurement results and BNL's was not acceptable.

This section reports the magnetic field adjustments of the 1.5 m IVU for Frontier Macromolecular Crystallography (FMX) beam-line. The magnetic performances of this device, such as first and second field integrals, electron orbit deviations and phase error have been examined at various gap values. As shown in the Fig. 2 the vertical magnetic peak field distribution before correction (red dots) measured at gap 6.2 mm presents an unusual amplitude modulation. The magnetic field variation is of 2.2% and the absolute residual field error is about of 50 G, omitting 4 end-peaks at each end of the device. Hall probe scans performed with the gap fully opened to 40 mm and 3.1 mm above the lower platen and below the upper platen confirms this sinusoidal modulation in the peak field distribution in both magnetic girder. It is mainly due to the gap deformations along the undulator axis, which cause a large rms phase error of about 8.8°. In order to compensate the gap variation and consequently to optimize the magnetic peak field and the resultant phase error increase, external gap adjustments have been performed by fine adjusters attached to the shafts connecting in-vacuum platens and out-of-vacuum girders as shown in Fig. 1. This mechanical adjustment is based on a differential adjuster developed at SPring-8 [9]. The gap correction has been achieved by monitoring the field change with the Hall probe located at the position of the shaft to be adjusted.

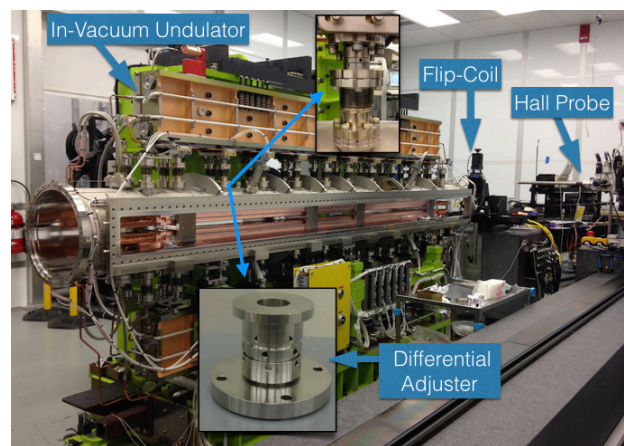


Figure 1: Magnetic retuning of an IVU at BNL IDs Lab.

Fig. 2 shows the vertical peak field distribution after correction (green dots). It is evident a significant improvement of the field quality and phase error. The RMS phase error after correction is thus reduced to 2.2°. Loss of spectral brightness is well correlated with the optical phase error, especially at high harmonics of the

Content from this work may be used under the terms of the CC BY 3.0 licence (© 2015). Any distribution of this work must maintain attribution to the author(s), title of the work, publisher, and DOI.

radiation as shown in Fig. 3, where the radiation spectrum of single-electron emission before and after magnetic adjustments has been calculated from the magnetic measurements.

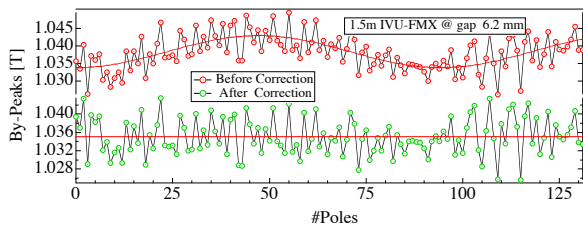


Figure 2: Vertical peak field distribution measured at gap 6.2 mm before (red dots) and after (green dots) magnetic correction.

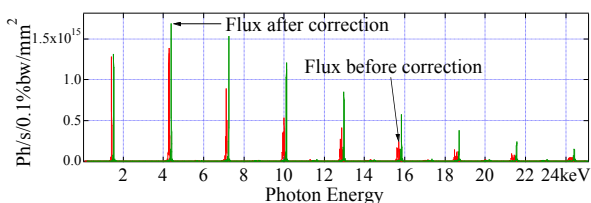


Figure 3: Radiation spectrum before (red line) and after (green line, with 100 eV offset) magnetic correction.

Additional corrections by magic finger were carried out in order to reduce the residual field integral errors and minimize the electron beam deflection from the nominal axis. Angular variations confined around 5 μ rad and maximum horizontal and vertical displacements of few microns have been achieved.

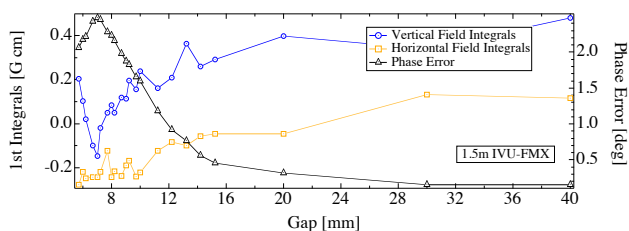


Figure 4: First vertical (blue line) and horizontal (orange line) field integrals and phase error (black line) as function of the gap.

Fig. 4 shows the first field integrals and phase error after magnetic tuning for each gap. From these results, we can conclude that the methods applied to correct the magnetic field are effective not only at the gap of optimization but also at larger gap values.

Commissioning Results

Table 2 shows the comparison between the measured 1st integrals ΔI_x and ΔI_y and those estimated from the electron beam, eI_x and eI_y , by measuring the close orbit distortion without any feedback when the undulator's gap is closed. X_{rms} and Y_{rms} are RMS values of difference between the measured orbit and simulated.

Table 2: Integrals Versus Estimated Values from e-beam

Device	Gap [mm]	ΔI_x [Gcm]	ΔI_y [Gcm]	eI_x [Gcm]	eI_y [Gcm]	X_{rms} Y_{rms} [μ m]
IVU20 HXN	6.7	-105.7	77.6	-11.1	-3.4	1.15
						0.50
IVU20 CHX	6.7	-33.3	11.6	17.9	32.5	1.19
						0.59
IVU21 SRX	6.5	-170.1	259.0	-81.2	88.9	1.99
						2.79
IVU22 IXS	6	17.7	214.8	-24.2	-15.9	2.42
						1.19

More studies are planned in order to investigate the unsatisfactory correlation between the measured first integrals and those estimated from electron beam. Misalignment during installation, Earth's magnetic field and interactions with environmental field, such as those arising from the existence of ferromagnetic structures nearby and stray magnetic field from other components could be responsible of this discrepancy.

CONCLUSION

After the magnetic adjustments and the magic finger corrections the devices have been achieved field characteristics of very high quality.

REFERENCES

- [1] F. Willeke, "Status of the NSLS-II Project," TUOBS3, PAC 2011, NY, USA.
- [2] T. Tanabe et al., "Insertion Devices at the National Synchrotron Light Source-II", Proc. SRI 2015, NY, USA.
- [3] F. Willeke, "Commissioning Results of NSLS-II", this conference IPAC'15, Richmond, VA, USA.
- [4] G. Wang et al., "NSLS-II Storage Ring Insertion Devices and Front-End Commissioning", this conference IPAC'15, Richmond, VA, USA.
- [5] M. Musardo et al., "NSLS-II Magnetic Measurement System Facility", PAC2013, Pasadena, CA, USA, (2013).
- [6] M. Musardo et al., "3D Hall Probe Calibration System at Insertion Device Magnetic Measurement Facility at BNL", PAC2013, Pasadena, CA, USA, (2013).
- [7] M. Musardo et al., "A new data acquisition software and analysis for accurate magnetic field integral measurement at BNL insertion devices laboratory", PCaPAC 2014, Karlsruhe, Germany (2014).
- [8] R. P. Walker, "Phase errors and their effect on undulator radiation properties", Phys. Rev. ST Accel. Beams 16 2013.
- [9] T. Tanaka et al., Phys. Rev. ST-AB 12 (2009) 120702.